How to Disassemble a Virus Capsid
A Computational Approach

Claudio Alexandre Piedade, António E. N. Ferreira and Carlos Cordeiro
Laboratório de FTICR e Espectrometria de Massa Estrutural, Centro de Química e Bioquímica, Departamento de Química e Bioquímica, Faculdade de Ciências, Universidade de Lisboa, 1749-016 Lisboa, Portugal

Keywords: Virus, Capsid Disassembly, Combinatorial Geometry, Symmetry Groups, Structural Biology.

Abstract: In contrast with the assembly process of virus particles, which has been the focus of many experimental and theoretical studies, the disassembly of virus protein capsids, a key event during infection, has generally been overlooked. Although the nature of the intracellular triggers that promote subunit disassembly may be diverse, here we postulate that the order of subunit removal is mainly determined by each virus structural geometry and the strength of subunit interactions. Following this assumption, we modelled the early stages of virus disassembly of $T = 1$ icosahedral viruses, predicting the sequence of removal of up to five subunits in a sample of 51 structures. We used combinatorics and geometry, to find non-geometrically identical capsid fragments and estimated their energy by three different heuristics based on the number of weak inter-subunit contacts. We found a main disassembly pathway common to a large group of viruses consisting of the removal of a triangular trimer. Densoviruses lose a square-shaped tetramer while Human Adenoviruses lose a pentagon-shaped pentamer. Results were virtually independent of the heuristic measure used. These findings suggest that particular subunit interactions might be an important target for novel antiviral drugs designed to interfere with capsid disassembly.

1 INTRODUCTION

Viruses are intracellular parasites that replicate inside living cells, by using its genetic and protein synthesis machinery to create new copies (Poranen et al., 2002; Mateu, 2013). Viral particles are composed by a nucleic acid (DNA or RNA, single or double stranded) and, in many cases, a capsid, a proteic structure that protects the genetic information in between infections (Caspar and Klug, 1962; Poranen et al., 2002; Prasad and Schmid, 2012). Round-shaped viruses have a fixed number of proteins or asymmetric units surrounding the genetic material in a icosahedral symmetry (Caspar and Klug, 1962; Prasad and Schmid, 2012). This arrangement was first described by Caspar and Klug in 1962, who developed a method to classify the icosahedral symmetry by triangulating the icosahedron facets. The Triangulation number (or T-number) represents the number of equilateral triangles that compose a triangular face of the icosahedron (Prasad and Schmid, 2012).

Many studies have addressed the virus assembly process, both experimentally and theoretically (reviewed in (Perlmutter and Hagan, 2015) and (Mateu, 2013)). Viruses' capsid subunits are held together by non-covalent interactions (Zlotnick, 1994; Zlotnick et al., 1999; Zlotnick, 2003) such as electrostatic salt bridges, hydrophobic contacts and hydrogen bonds. The effects of a myriad of these weak interactions is a globally stable capsid (Zlotnick and Stray, 2003). Virus assembly is spontaneous *in vitro* under close-to-physiological conditions (Mateu, 2013) and the resulting capsids are stable for a long period of time. Results derived from theoretical models of virus assembly consistently agree on the prediction that three trimeric protomers, pentamers of trimers and capsids with just a triangular icosahedron face missing are stable intermediate forms that precede the formation of a complete capsid (Zlotnick, 1994; Zlotnick et al., 1999; Reddy et al., 1998; Reddy and Johnson, 2005; Rapaport, 2008; Rapaport, 2010). If capsid disassembly was just the reverse process of capsid assembly, these finding would suggest that the same structures would be found during disassembly. In high contrast to the number of studies focusing on the assembly process, there are very few experimental studies on capsid disassembly pathways. Since it is expected that intermediates of this process are transient and very difficult to detect experimentally, models of the disassembly pathways are always difficult to confirm

Piedade C., Ferreira A. and Cordeiro C.
How to Disassemble a Virus Capsid - A Computational Approach.
DOI: 10.5220/0006249802170222
In *Proceedings of the 10th International Joint Conference on Biomedical Engineering Systems and Technologies (BIOSTEC 2017)*, pages 217-222
ISBN: 978-989-758-214-1

experimentally. Moreover, the assembly and disassembly pathways might not be symmetric since some viruses undergo maturation steps after assembly completion, such as proteolysis, cross-linking or conformational change (Zlotnick and Stray, 2003). Castellanos et al. (Castellanos et al., 2012), using Atomic Force Microscopy (AFM), observed the removal of a triangle of subunits (an icosahedral face) when force was applied over the Minute Virus of Mice, followed sometimes by the loss of an adjacent triangle. In other cases, a removal of a pentamer of triangles (15 proteins) was observed. This follows the predictions of the assembly models (Reddy et al., 1998; Reddy and Johnson, 2005; Rapaport, 2008; Rapaport, 2010). Horton and Lewis (Horton and Lewis, 1992) stated that the energy minimums appear every multiple of three subunits. Ortega-Esteban et al. (Ortega-Esteban et al., 2013) have shown also by AFM that for Human Adenoviruses the disassembly, both for mature and immature capsids, start by the loss of a pentagon of proteins.

The work described here tackles the lack of theoretical studies targeting the disassembly process relying on rigorous geometrical and combinatorial considerations, focusing primarily on $T = 1$ icosahedral capsid structures. This work in progress has the long-term goal of providing insights into the disassembly process, which can be used in the development of antiviral drugs interfering with intermediate states of the process.

2 METHODS

2.1 Combinatorics and Symmetry

Virus capsid structures with $T = 1$, although having icosahedral symmetry, are not icosahedron-like, as they contain 60 proteins instead of only 20. The 60-face polyhedron, in which each triangular face of the icosahedron is divided into three faces, is the Deltoidal Hexecontahedron. Due to the symmetry of the Deltoidal Hexecontahedron, the combinations of removing N proteins from a capsid ($\binom{60}{N}$) leads to redundancy since some are symmetrically equivalent, and the real number is smaller. The exact number of combinations can be obtained by studying the Burnside's Lemma (Burnside, 1909). To build up the group of permutations associated with the rotations of a Deltoidal Hexecontahedron, the faces were numbered as shown in Figure 1, followed by the analysis of the transformations done on the numbering of the faces by the symmetry operators of the symmetry group I (Vincent, 2001). Applying the different

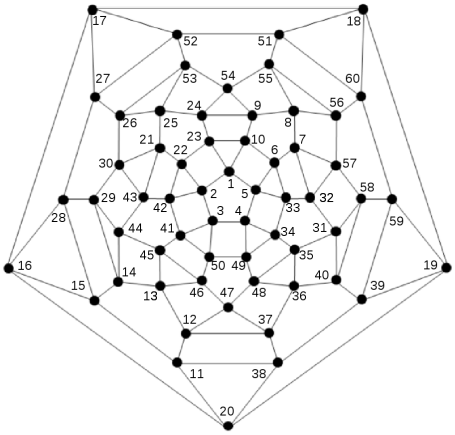

Figure 1: Graph representation of the Rhombicosidodecahedron. Each vertex represents a subunits of the $T = 1$ virus capsid. Edges represent geometrical edges.

rotations on the symmetry axes of a Deltoidal Hexecontahedron, results in a permutation group. These permutations can be seen as permutations of faces of the Deltoidal Hexecontahedron or vertices of its dual, the Rhombicosidodecahedron. Since the graph of a Rhombicosidodecahedron (Figure 1) allows the study of each protein as a vertex, in what follows we mainly used that perspective to develop the following methods of the analysis of virus disassembly.

2.2 Structures of Viruses' Capsids

Capsids' atomic coordinates were obtained from the Protein Data Bank (*PDB*, http://www.rcsb.org/, (Berman et al., 2000)). Only $T = 1$ capsids, present on ViperDB were considered (http://viperdb.scripps.edu, (Carrillo-Tripp et al., 2009)). The capsid structures analysed in this work were divided into groups according to the criteria of similarity of the infection host and the genes codifying capsid proteins. The list is presented in Table 2, with 51 structures divided into 14 groups. Human Adenovirus are mainly $T = 25$ and the structures studied here are a stable capsid formed with the pentagons of the $T = 25$, forming a Dodecahedron (named from now on as Human Adenovirus Pt-Dd or HAPD).

2.3 Energy Calculation

To calculate the energy of the full capsid and its disassembly products, the number of hydrogen bonds, salt bridges and hydrophobic contacts between capsid subunits were counted (intra-protein contacts were ignored). Hydrogen bonds (N_{HB}) were counted if acceptor and donor's atoms indicated in Table 1 were

Table 1: Donor and Acceptor's Atoms used to calculate Hydrogen Bonds.

	Amino acids
Donor	ARG(N_ε; $N_{\eta 1}$; $N_{\eta 2}$), ASN($N_{\delta 2}$), CYS(S_γ), GLN($N_{\varepsilon 2}$), HIS($N_{\delta 1}$; $N_{\varepsilon 2}$), LYS(N_ζ), SER(O_γ), THR($O_{\gamma 1}$), TRP($N_{\varepsilon 1}$), TYR(O_η)
Acceptor	ASN($O_{\delta 1}$), ASP($O_{\delta 1}$; $O_{\delta 2}$), GLN($O_{\varepsilon 1}$), GLU($O_{\varepsilon 1}$; $O_{\varepsilon 2}$), HIS($N_{\delta 1}$; $N_{\varepsilon 2}$), SER(O_γ), THR($O_{\gamma 1}$), TYR(O_η)

at a distance less than or equal to 4.0Å. A salt bridge bound (N_{SB}) was counted if a positively charged atom of an acidic amino acid (ASP and GLU) was found within 4.0Å of a negatively charged atom of a basic amino acid (ARG and LYS). A hydrophobic contact (N_{HC}) was counted when β-carbons of the residues ALA, VAL, LEU, ILE, MET, PHE, TYR and TRP, were found at the distance less than or equal to 7.0Å. We can calculate a heuristic measure of total energy of a complete capsid or capsid fragment (Equations (1) to (3)).

$$E_1 = N_{SB} + N_{HB} + N_{HC} \quad (1)$$

$$E_2 = 20 \times N_{SB} + N_{HB} + N_{HC} \quad (2)$$

$$E_3 = 100 \times N_{SB} + 10 \times N_{HB} + N_{HC} \quad (3)$$

In Heuristic I (Equation (1)), only the total number of inter-subunit bonds in the capsid complex is taken into account; the three types of bounds are equally weighted. Heuristic II (Equation (2)) gives Salt Bridges 20 times more energy than Hydrogen Bonds. Hydrophobic Contacts was considered to be energetically equivalent to making Hydrogen Bonds, since a water "cage" is destroyed when hiding hydrophobic amino acids, breaking Hydrogen Bonds made by the water itself to hold this cage (Atkins and De Paula, 2006). On the other hand, on Heuristic III (Equation (3)) an increasing power of 10 was given to each type of inter-subunit bond, in the known order of strength of this types of contacts (Salt Bridges > Hydrogen Bonds > Hydrophobic Contacts) (Atkins and De Paula, 2006).

2.4 Removal of Proteins and Graph Representation

Each possible capsid fragment can be represented by a 60 element binary vector, depending on the presence or absence of each protein given the subunit numbering of Figure 1. A list of non-redundant binary vectors representing capsid fragments was then obtained as follows: for every combination of N indexes of a size 60 vector, a binary vector was generated with zeros in those positions and ones elsewhere; permutations of the permutation group mentioned above were applied to this vector; if any of the resulting vectors was not identical to another previously obtained it would be appended to the list. Thus, a set of non geometrically identical capsid fragments was obtained. Their representation as a subgraph of Figure 1 allowed us to check if disconnected fragments were obtained at each step, so that the largest fragment was retained and the search for non redundant forms was also applied to this fragment. Finally, the fragment's the energy was calculated according to each heuristic.

2.5 Optimal Path for Disassembly

For all the possibilities of removing N proteins, a tree of all the paths that the virus disassembly process could take was built, rooted at the intact virus capsid ($N = 0$). Edges were given a transition energy weight, based on the average heuritic energy per protein, following Equation 4. The size of configuration i is equal to $60 - N_i$, where N_i was the number of proteins removed.

$$E_{transition\ i \to j} = \frac{E_j}{size_j} - \frac{E_i}{size_i} \quad (4)$$

The Bellman-Ford algorithm was used on this tree to calculate the shortest path from the complete viral capsid to every possibility of a capsid with $60 - N$ proteins, based on the weights of the edges of the tree, recording the five shortest paths for every N and the corresponding final configuration.

2.6 Implementation

All methods were implemented in Python 2.7 using scientific computing modules (igraph Python bindings (Csardi and Nepusz, 2006)). All the code is available on GitHub repository: https://github.com/CAPiedade/Virus-Disassembly.

3 RESULTS AND DISCUSSION

The disassembly paths of the different capsids are portrayed in Table 2 considering heuristic I. It can be observed that most Parvoviruses (marked with a †) follow the same sequence of disassembly: $\{1\} \to \{1,10\} \to \{1,10,23\} \to \{1,2,10,23\} \to \{1,2,10,22,23\}$. Fragment $\{1,10,23\}$ represents the removal of a triangle of proteins on the capsid structure (Figure 2.A). As observed in the mechanical removal of proteins with AFM (Castellanos et al., 2012), the Minute Mice Virus (on our work represented by the group of the Rodent Protoparvovirus)

Table 2: Capsid groups and minimal energy paths taken to reach the removal of N subunits using heuristic I. Viruses marked with † are Parvoviruses (Family *Parvoviridae*).

	N				
Groups	**1**	**2**	**3**	**4**	**5**
Adeno-Associated Virus† (3j4p, 3ra8, 4iov, 3j1q, 3ntt, 3ra2, 3ux1, 2g8g, 1lp3, 2qa0, 3ra4, 3ra9, 3raa, 4rso, 5egc)	$\{1\}$	$\{1,10\}$	$\{1,10,23\}$	$\{1,2,10,23\}$	$\{1,2,10,22,23\}$
Bovine Parvovirus† (4qc8)					
Human Parvovirus† (1s58)					
Porcine Parvovirus† (1k3v)					
Canine and Feline Panleukopenia Virus† (1c8f, 1c8h, 1c8e, 1c8g, 1fpv, 1p5y, 1c8d, 1p5w, 4dpv, 1ijs, 2cas)				$\{1,9,24,54\}$ $\{1,2,10,23\}$	
Rodent Protoparvovirus† (1mvm, 1z14, 4g0r, 1z1c, 2xgk, 4gbt)				$\{1,2,10,23\}$	
Avian Birnavirus (1cwd)					
Porcine Circovirus (3r0r, 3jci)				$\{1,2,22,42\}$ $\{1,2,10,23\}$	
Bombyx mori Densovirus† (3p0s)		$\{1,2\}$		$\{1,2,22,23\}$	
Galleria mellonella Densovirus† (1dnv)					
Penaeus stylirostris Densovirus† (3n7x)			$\{1,2,23\}$		$\{1,2,6,10,23\}$
Satellite Tobacco Mosaic Virus (2buk, 4bcu, 1a34, 4oq8)		$\{1,6\}$	$\{1,2,6\}$ $\{1,2,23\}$	$\{1,2,6,7\}$ $\{1,2,6,24\}$ $\{1,2,6,23\}$	$\{1,2,6,10,24\}$ $\{1,2,3,23,42\}$ $\{1,2,6,10,23\}$
Hepatitis E Virus (HEV) (2ztn, 2zzq, 3hag)			$\{1,2,23\}$	$\{1,2,10,23\}$ $\{1,2,6,23\}$	$\{1,2,6,10,23\}$
Human Adenovirus Pt-Dd (1x9t, 4aqq, 4ar2)		$\{1,2\}$	$\{1,2,3\}$	$\{1,2,3,4\}$	$\{1,2,3,4,5\}$

tends to start the disassembly process by losing a triangular block, which is then followed by the removal of the adjacent triangle. This is supported by our results since most disassembly pathways lead to the removal of a triangular structure, commonly composed of proteins $\{1,10,23\}$. The theoretical studies of Rapaport et al. (Rapaport, 2008; Rapaport, 2010) reveal the existence of long-lived transient structures with just one last triangle of proteins missing to form the complete capsid. The results of Reddy et al. (Reddy et al., 1998) using both individual proteins and trimers show the same for capsid assembly (Reddy et al., 1998), suggesting that the path for disassembly also follows the triangle removal. Fragment $\{1,2,10,22,23\}$ represents the removal of a trapezium-like shape, centred on the triangle $\{1,10,23\}$ (Figure 2.C) Supposing this trend continues, it is not hard to see that there is a chance of removing the proteins around the five-fold axis. These could be the follow up steps of the disassembly of these capsids, potentially resulting in the loss of 15 proteins such as $\{1,2,3,4,5,6,10,22,23,33,34,41,42,49,50\}$. Castellanos et al.'s results confirms the predictions of Reddy et al. (Reddy et al., 1998), since the lowest energy configuration, just before the complete capsid, was missing a pentamer of triangles (corresponding to the 15-protein combinations described before), inclusively for Parvoviruses (Reddy and Johnson, 2005). The removal of four proteins has more than one possibility. Most parvoviruses lose subunits $\{1,2,10,23\}$ (Figure 2.B). Densovirus, on the other hand, tend to lose proteins $\{1,2,22,23\}$, a configuration leading to a square hole on the two-fold symmetry of the capsid (Figure 2.D). We might speculate that the inter-subunit interactions on these viruses are different from the others parvoviruses. To verify this, we took the ratio between the number of intersubunit contacts $[22 \leftrightarrow 23]$ and the number of intersubunit contacts $[10 \leftrightarrow 23]$, the only two interactions between capsid proteins that are different between $\{1,2,22,23\}$ and the common parvovirus structure $\{1,2,10,23\}$, respectively. These results are shown on Table 3, where it can be observed that Parvoviruses have a lower ratio than Densovirus, suggesting that

$$\#[22\leftrightarrow 23]/\#[10\leftrightarrow 23] > 0.82 \Rightarrow \{1,2,22,23\}$$

$$\#[22\leftrightarrow 23]/\#[10\leftrightarrow 23] < 0.80 \Rightarrow \{1,2,10,23\}$$

Further analysis of these and other ratios will provide some insight into why some structures are oriented into particular pathways. Removing of a square-shaped group of proteins raises the idea that the higher the symmetry of the structures removed, the higher is their chance to be lost. Structures with PDB_{ID} 1c8f and 1c8h differ only inside its group for the removal of the four proteins $\{1,9,24,54\}$. Avian Birnavirus follow the same path as the majority of Parvovirus, as well as Porcine Circovirus, with the exception of structure with PDB_{ID} 3jci which loses $\{1,2,22,42\}$,

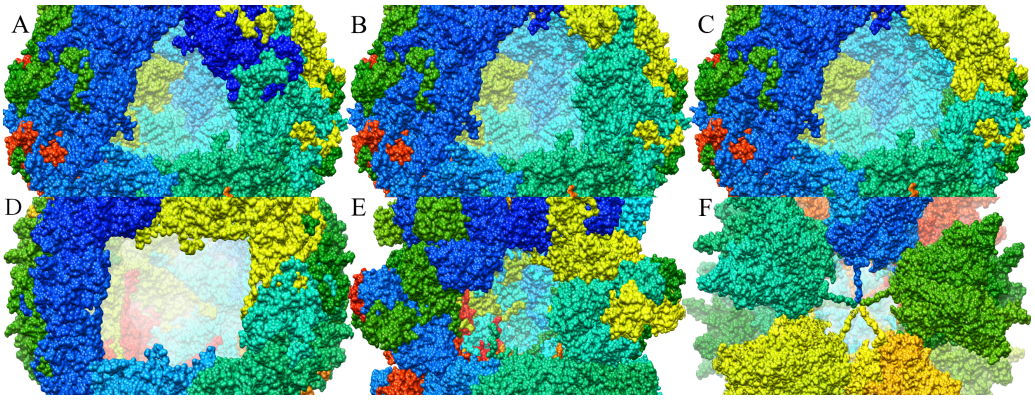

Figure 2: Disassembly stages of different viruses. Parvoviruses (PDB_{ID} 1s58) path $\{1,10,23\}$ (A), $\{1,2,10,23\}$ (B) and $\{1,2,10,22,23\}$ (C). Densovirus (PDB_{ID} 1dnv) path $\{1,2,22,23\}$ (D). HEV (PDB_{ID} 2zzq) path $\{1,2,6,10,23\}$ (E). HAPD (PDB_{ID} 4aqq) path $\{1,2,3,4,5\}$ (F). Structures are represented showing molecular surfaces. UCSF Chimera (Pettersen et al., 2004) was used for rendering.

Table 3: Ratio of contacts between proteins #[22 ↔ 23] and #[10 ↔ 23].

Ratio of the number of contacts	Densovirus			Parvovirus	
	1dnv	3n7x	3p0s	1s58	3raa
$^{\#[22\leftrightarrow 23]}/_{\#[10\leftrightarrow 23]}$	$^{18}/_{19} \approx 0,95$	$^{15}/_{11} \approx 1,36$	$^{23}/_{28} \approx 0,82$	$^{35}/_{44} \approx 0,80$	$^{35}/_{62} \approx 0,56$

a reflection of $\{1,2,10,23\}$. HEV capsids loses proteins on the order $\{1\} \rightarrow \{1,6\} \rightarrow \{1,2,23\} \rightrightarrows \{1,2,6,23\} \rightrightarrows \{1,2,6,10,23\}$. Although distinguishable from the Parvovirus, HEV loses a pentamer that forms a triangular hole on the capsid structure (Figure 2.E). HAPD follows the disassembly path $\{1\} \rightarrow \{1,2\} \rightarrow \{1,2,3\} \rightarrow \{1,2,3,4\} \rightarrow \{1,2,3,4,5\}$, an exception to all the others. The Human Adenovirus group is the only undergoing a five-fold removal of the proteins, removing the pentamer $\{1,2,3,4,5\}$ (Figure 2.F). On Figure 2.F we can observe the structure of a HAPD, which is formed by very condensed clusters of pentagons, having very few contacts with the 2-fold and 3-fold proteins. The distance between the pentagonal clusters on the full capsid structure might make it easier for this set of subunits to be removed, in opposition to creating a bigger gap by removing, for example, proteins $\{1,2,10,22,23\}$. Our results are supported by those of Ortega-Esteban et al. (Ortega-Esteban et al., 2013) which showed, through AFM, a loss of a pentagon-shaped pentamer of proteins for Human Adenoviruses. Satellite Mosaic Tobacco Virus disassembly was to diverse. The results from this group were not analysed any further since due to the small size of the set.

We also investigated the effect of the other two heuristics (Equations 2 and 3). Results were very similar to heuristic I, with a slightly higher degree of branching. Nevertheless, the loss of three and five proteins was conserved in all heuristics.

4 CONCLUSIONS

Our study began with the goal of investigating whether there was a common disassembly pathway among different virus families and, if not, if there would be a conserved disassembly path for each family. Results on this work support the idea that, for a large cluster of $T = 1$ viruses, there is a common disassembly pathway. This cluster is composed by some Parvoviruses (Adeno-Associated Virus, Bovine Parvovirus, Human Parvovirus, Porcine Parvovirus, Rodent Protoparvovirus, Canine and Feline Panleukopenia Virus), Avian Birnavirus, Hepatitis E Virus and Porcine Circovirus. From our results, we can speculate that the results of Castellanos et al. (Castellanos et al., 2012) might be applicable to more families of viruses besides the Rodent Protoparvovirus. Densoviruses (from *Bombyx mori*, *Galleria mellonella* and *Penaeus stylirostris*) are exceptional for their exclusive removal of proteins $\{1,2,22,23\}$, with no branching to alternative possibilities. On the other hand, Human Adenoviruses have a very particular pathway of disassembly, establishing that not all disassemblies proceed through the removal of triangular protein trimers, but also through the removal of protein pentagons. Using a combinatorial method based on symmetry and geometry, with a 60-subunit model (Deltoidal Hexecontahedron) and not a 20-subunit model (Icosahedron) or 12-subunit model (Dodecahedron), under a heuristic using the number of weak

contacts, we obtained results comparable to those found in previous literature. Furthermore, the usage of a 60-subunit model allows the study of cases such as those of Human Adenoviruses, which do not lose triangular faces of the Icosahedron, but a pentagon of faces of the Deltoidal Hexecontahedron. Nonetheless, an increase of the sample size is an important follow-up step, since it would give a better insight into the trends observed for the different viruses studies. Moreover, the number of subunits removed from the capsid structures should be above 5 to offer a perspective of what would be the next steps on the disassembly pathway. Improvement of the algorithms as well as the processing power could provide more informative results beyond 5. Understanding the way viruses' capsids disassemble can be used to interfere with the inter-subunit interactions, specially those who hold the triangular trimer in the complete capsid. Antiviral drugs can thus be design to disrupt these interactions.

ACKNOWLEDGEMENTS

Work supported by project RECI/BBB-BEP/0104/2012 from Fundação para a Ciência e Tecnologia, Portugal. The funders had no role in study design, data collection and analysis, decision to publish, or preparation of the manuscript.

REFERENCES

Atkins, P. W. and De Paula, J. (2006). *Physical chemistry for the life sciences*. Oxford University Press ; W.H. Freeman, Oxford, UK : New York.

Berman, H. M., Westbrook, J., Feng, Z., Gilliland, G., Bhat, T. N., Weissig, H., Shindyalov, I. N., and Bourne, P. E. (2000). The protein data bank. *Nucleic acids research*, 28(1):235–242.

Burnside, W. (1909). Theory of groups of finite order. *Messenger of Mathematics*, 23:112.

Carrillo-Tripp, M., Shepherd, C. M., Borelli, I. A., Venkataraman, S., Lander, G., Natarajan, P., Johnson, J. E., Brooks, C. L., and Reddy, V. S. (2009). Viperdb2: an enhanced and web api enabled relational database for structural virology. *Nucleic acids research*, 37(suppl 1):D436–D442.

Caspar, D. L. D. and Klug, A. (1962). Physical Principles in the Construction of Regular Viruses. *Cold Spring Harbor Symposia on Quantitative Biology*, 27(0):1–24.

Castellanos, M., Prez, R., Carrillo, P., dePablo, P., and Mateu, M. (2012). Mechanical Disassembly of Single Virus Particles Reveals Kinetic Intermediates Predicted by Theory. *Biophysical Journal*, 102(11):2615–2624.

Csardi, G. and Nepusz, T. (2006). The igraph software package for complex network research. *InterJournal*, Complex Systems:1695.

Horton, N. and Lewis, M. (1992). Calculation of the free energy of association for protein complexes. *Protein Science*, 1(1):169–181.

Mateu, M. G. (2013). Assembly, stability and dynamics of virus capsids. *Archives of Biochemistry and Biophysics*, 531(1-2):65–79.

Ortega-Esteban, A., Prez-Bern, A. J., Menndez-Conejero, R., Flint, S. J., Martn, C. S., and de Pablo, P. J. (2013). Monitoring dynamics of human adenovirus disassembly induced by mechanical fatigue. *Scientific Reports*, 3.

Perlmutter, J. D. and Hagan, M. F. (2015). Mechanisms of Virus Assembly. *Annual Review of Physical Chemistry*, 66(1):217–239.

Pettersen, E. F., Goddard, T. D., Huang, C. C., Couch, G. S., Greenblatt, D. M., Meng, E. C., and Ferrin, T. E. (2004). Ucsf chimeraa visualization system for exploratory research and analysis. *Journal of computational chemistry*, 25(13):1605–1612.

Poranen, M. M., Daugelaviius, R., and Bamford, D. H. (2002). Common Principles in Viral Entry. *Annual Review of Microbiology*, 56(1):521–538.

Prasad, B. V. V. and Schmid, M. F. (2012). Principles of Virus Structural Organization. In Rossmann, M. G. and Rao, V. B., editors, *Viral Molecular Machines*, volume 726, pages 17–47. Springer US, Boston, MA.

Rapaport, D. C. (2008). Role of Reversibility in Viral Capsid Growth: A Paradigm for Self-Assembly. *Physical Review Letters*, 101(18).

Rapaport, D. C. (2010). Studies of reversible capsid shell growth. *Journal of Physics: Condensed Matter*, 22(10):104115.

Reddy, V. S., Giesing, H. A., Morton, R. T., Kumar, A., Post, C. B., Brooks, C. L., and Johnson, J. E. (1998). Energetics of Quasiequivalence: Computational Analysis of Protein-Protein Interactions in Icosahedral Viruses. *Biophysical Journal*, 74(1):546–558.

Reddy, V. S. and Johnson, J. E. (2005). Structure-Derived Insights into Virus Assembly. In *Advances in Virus Research*, volume 64, pages 45–68. Elsevier.

Vincent, A. (2001). *Molecular symmetry and group theory: a programmed introduction to chemical applications*. Wiley, Chichester ; New York, 2nd ed edition.

Zlotnick, A. (1994). To build a virus capsid. An equilibrium model of the self assembly of polyhedral protein complexes. *J. Mol. Biol.*, 241(1):59–67.

Zlotnick, A. (2003). Are weak proteinprotein interactions the general rule in capsid assembly? *Virology*, 315(2):269–274.

Zlotnick, A., Johnson, J. M., Wingfield, P. W., Stahl, S. J., and Endres, D. (1999). A theoretical model successfully identifies features of hepatitis B virus capsid assembly. *Biochemistry*, 38(44):14644–14652.

Zlotnick, A. and Stray, S. J. (2003). How does your virus grow? Understanding and interfering with virus assembly. *Trends Biotechnol.*, 21(12):536–542.